Received: 15 February 2022 | Revised: 28 May 2022 | Accepted: 25 July 2022

DOI: 10.1002/pen.26102

RESEARCH ARTICLE

POLYMER ENGINEERING AND SCIENCE WILEY

Origin of the broad endothermic peak observed at low temperatures for polystyrene and metals in Flash differential scanning calorimetry*

Madhusudhan R. Pallaka[1] | **Rozana Bari**[1] | **Sindee L. Simon**[2]

[1]Department of Chemical Engineering, Texas Tech University, Lubbock, Texas, USA

[2]Department of Chemical and Biomolecular Engineering, North Carolina State University, Raleigh, North Carolina, USA

Correspondence
Sindee L. Simon, Department of Chemical and Biomolecular Engineering, North Carolina State University, Raleigh, NC 27695, USA.
Email: slsimon@ncsu.edu

Funding information
National Science Foundation, Grant/Award Numbers: DMR-2141221, DMR-2004960

*Gregory B. McKenna Virtual Issue

Abstract

The glass transition behavior of polystyrene as a function of different cooling rates with scanning to two different end temperatures, 30°C and −80°C, was investigated for four different substrate conditions using Flash differential scanning calorimetry, a fast scanning nanocalorimetry technique. In addition, structural recovery of polystyrene was performed at 20°C for aging times from 0.01 s to 8 h with scanning to −80°C for the same samples. A broad endotherm appears to grow at low temperatures ($T << T_g$) as cooling rate decreases and aging time increases, which is influenced by the substrate underlying the film, as well as by the end temperature condition in the scanning experiment. On the other hand, the endothermic overshoot associated with T_g is not influenced by substrate or scan end temperature. In addition, indium and vapor-deposited gold, both crystalline materials, show the growth of a very similar broad endotherm at low temperatures as cooling rate decreases and aging time increases indicating that the low-temperature endotherm is an artifact and not a relaxation associated with the material under investigation. Several potential explanations are put forward.

KEYWORDS
calorimetry, glass transition, polystyrene

1 | INTRODUCTION

The appearance of a broad low-temperature endothermic overshoot has been observed for polymers in the glassy state ($T << T_g$), both at nano and micron scale alike, when studied using Flash differential scanning calorimetry (DSC).[1-3] The low-temperature endotherms of micrometer thick poly(4-tert butylstyrene) films demonstrated a cooling rate dependence, with the area of the endotherm increasing with decreasing cooling rate.[1,2] In addition, a low-temperature broad endotherm was also observed for polystyrene nanospheres,[3] with the area of the endotherm increasing with aging time and decreasing aging temperature during structural recovery studies; intermediate plateaus were also observed during the relaxation process. The presence of a low-temperature

Madhusudhan R. Pallaka and Rozana Bari are co-first authors.

endotherm has been attributed by Cangialosi and coworkers[1,3-6] as a fast relaxation at temperatures $T << T_g$ which can be exploited, for example, to attain very low-fictive temperature glasses. In addition to the studies using Flash differential scanning calorimetry, low-temperature endotherms were also observed in case of structural recovery studies ($T_a << T_g$) of various glassy polymers using conventional DSC. Room temperature aging of three polymers, poly(acrylate), poly(bisphenol-A-carbonate), and polysulfone showed aging plateau between aging times of 60 days to 30 years due to the presence of a low-temperature endotherm.[5] Stacked polystyrene thin films with thicknesses in the range of 30–95 nm also exhibited broad low-temperature endotherms contributing to the two-step structural recovery process.[4,6]

The existence of an endotherm at low temperatures for glassy polymers is certainly controversial due to the lack of systematic studies. We hypothesize that the phenomenon is an artifact, potentially arising from residual stresses rather than due to the inherent properties of the material under investigation. Hence, in this study, we investigate the existence and consistency of the broad low-temperature endotherms by performing cooling rate dependent and room temperature aging experiments using Flash DSC, a relatively new fast scanning nanocalorimetry technique that has the advantages of covering over five decades in cooling rates, including rates that are relevant to polymer processing, and the ability to characterize samples in the absence of degradation due to the rates.[7–9]

Here, we use the Flash DSC to investigate 1.3-micron thick polystyrene films atop different substrates including Krytox oil, an anodic aluminum oxide (AAO) template with 350 nm-diameter straight-walled pores (termed 350 nm AAO), an anodic aluminum oxide template with 55 nm pores (termed 55 nm AAO), and directly on the bare chip. The different substrates allow a systematic change of residual stresses in the sample with the direct contact case having the highest stress. In addition to the studies on glassy polystyrene, we also investigate the influence of the cooling rate and isothermal aging on crystalline metals, indium, and vapor-deposited gold at two different substrate temperatures, neither of which should have relaxations below T_m, to further probe the origin of the broad low-temperature endotherms.

2 | EXPERIMENTAL

2.1 | Materials and methodology

Two high molecular weight, atactic polystyrene samples (PS) (Scientific Polymer Products Inc., USA) were studied; one with a number-average molecular weight of 2,199,000 g/mol and a PDI of 1.04 was used to prepare thin films placed on the bare chip, Krytox oil, and 55 nm AAO template. The other with a number-average molecular weight of 2,100,000 g/mol and a PDI of 1.15 was used to prepare the thin film placed on 350 nm AAO.

PS thin films were prepared by spin-coating a 10 wt% solution of PS in toluene (99.999% purity, HPLC grade, Sigma-Aldrich) on hydrophilic silicon and mica substrates. The thicknesses of the thin films made were measured using an atomic force microscope (Agilent technologies) in tapping mode after making a scratch on the film; the thicknesses were measured to be as 1.3 ± 0.1 μm and 1.3 ± 0.3 μm for samples having molar masses of 2,199,000 and 2,100,000 g/mol, respectively. The PS thin films were placed on the Flash DSC sensors on top of four different substrates. In the case of PS films on Krytox oil and bare chip, PS thin films were cut directly from the silicon substrate (plasma treated to make it hydrophilic); one was placed directly on top of 30 ng Krytox oil (DuPont™) already present on the heating area of the chip sensor, and the other was transferred directly onto the chip heating area surface using a wire loop holding the film floating on a bead of water to prevent folding of the film, followed by drying for a week under desiccant.

Two AAO substrates with 5 μm thickness and pore diameters of 55 ± 2.0 (Synkera Technologies, USA) and 350 ± 45.0 nm (Universidad de Oviedo, Spain) were used to determine whether the underlying substrate influenced the presence of the low-temperature endotherm. Substrates were cut to the size of the Flash heating area, and a PS film was transferred to the top of the substrate after floating on water from the mica substrate and picking up with a wire mesh. Films were dried and then allowed to adhere to the template for 30 min at 120°C in a vacuum oven. The thicknesses of the AAO templates were limited to 5 μm to reduce thermal lag in the Flash DSC.[10,11]

Gold (Kurt J. Lesker Company, Purity: 99.99%) and indium (Mettler Toledo, Purity: 99%) were also studied on the Flash DSC. Gold of 50 ± 2 nm thick was vapor deposited on the heating area of the Flash DSC chip under vacuum at two different substrate temperatures (T_s), 23°C and 125°C. In the case of indium, a small pellet was flattened to ~1 μm thickness and placed on the heating area of the chip.

3 | METHODOLOGY

3.1 | Fast scanning nanocalorimetry

A Mettler Toledo Flash DSC 1 with a Freon intercooler maintained at −100°C was used to perform

TABLE 1 Material, substrate type or condition, and mass of samples studied

Material	Substrate type or condition	Sample mass (ng)
1.3 μm polystyrene film	Bare chip	154[a], 166[b]
	Krytox	96[a], 102[b]
	350 nm AAO	190[b]
	55 nm AAO	83[b]
50 nm gold	Vapor deposited at $T_s = 23°C$ on bare chip	120[a]
	Vapor deposited at $T_s = 125°C$ on bare chip	90[a]
Indium	Bare chip	176[c]

[a]Sample mass obtained from symmetry analysis.
[b]ΔC_p.
[c]ΔH_f.

measurements; a 20 ml/min nitrogen gas purge was used for an inert atmosphere. The chip sensors were conditioned and corrected according to the manufacturer's recommendation. To explore the low-temperature endothermic peak two different measurements were performed: (1) cooling rate dependent measurements and (2) structural recovery measurements. For the cooling rate dependent measurements, a heating scan was performed at 1000 K/s after cooling at various rates from 0.1 to 1000 K/s for two different scanning temperature ranges, −80°C to 190°C and 30°C to 190°C, for the polystyrene samples on the four different substrates and the 1 μm thick indium sample (T_m = 156.9°C); in the case of the 50 nm vapor deposited gold samples, the high-end temperature was 380°C instead of 190°C. Structural recovery experiments involved performing an aged scan at a heating rate of 1000 K/s from −80°C to 190°C (or 380°C for gold) after isothermally aging at 20.5°C for a prespecified time from 0.01 s to 8 h; all of the aged scans were followed by unaged scans.

Sample mass in Flash DSC is determined in several ways and involves comparing the heat flow or integrated heat flow area to known heat capacity or enthalpy values. In the case of the polystyrene films on the bare chip and Krytox oil and the vapor-deposited gold samples, mass was obtained by dividing the symmetry corrected heat flow[11,12] with the absolute liquid state heat capacity in the case of polystyrene[13,14] and absolute heat capacity in case of gold.[15] For all four polystyrene samples (on the bare chip, Krytox, and AAO), the mass of each was also obtained from the step change in heat flow measured at T_g and the change in heat capacity at T_g (ΔC_p) for a bulk polystyrene film defined in Equation (1)[16-18]:

$$\Delta C_p = 0.433 - 0.00148 T_f{}'(°C), \quad (1)$$

where T_f' is the limiting fictive temperature of a polystyrene sample for a cooling rate of 1000 K/s. The sample mass of indium was obtained by dividing the measured heat flow of melting with the enthalpy of melting.[19] The sample masses of all the samples are listed in Table 1 and ranged from 90 to 176 ng; for the polystyrene on the bare chip and Krytox oil, the first two methods give sample masses that are in good agreement. For the four polystyrene samples, we use the sample mass obtained by matching ΔC_p for the analyses to be consistent of our treatment between samples.

3.2 | Calculation of enthalpy change and fictive temperature

The enthalpy of a glass decreases as the cooling rate (q) decreases and as aging time (t_a) increases. This change in enthalpy relative to that in a reference state is obtained from Equation (2):

$$\Delta H = \frac{1}{m\beta}\int_{T_{low}}^{T_{high}} (\Delta \dot{Q})\, dT, \quad (2)$$

where m is the sample mass, β is the heating rate of 1000 K/s, and $\Delta\dot{Q}$ ($=\dot{Q}-\dot{Q}_{ref}$) is the difference in heat flow of a given heating scan (after cooling at some rate q or aging for some time t_a) and a reference unaged heating scan made after cooling at 1000 K/s. The integration limits, T_{high} and T_{low}, for all polystyrene measurements were varied to obtain the difference in the heat flow between the scan of interest and the unaged reference scan for the high-temperature area (related to the glass transition as explained later), and the total area (high-temperature area + low-temperature area) to study the evolution of the low-temperature endothermic peak. In the case of gold and indium (without a T_g), integration limits spanned the entire breadth of their respective measurements.

The limiting fictive temperature (T_f'), which is equivalent to T_g but is measured on heating, was determined from the superposed Flash DSC heating scans for the polystyrene samples after cooling at various rates between 0.1 to 1000 K/s by Moynihan's method[20] for cooling rates greater than 10 K/s and by a simplified form, Richardson's method,[21] for cooling rates less than 10 K/s where T_f' is lower than the onset of devitrification. The Moynihan's method and Richardson's method are defined here in terms of heat flow:

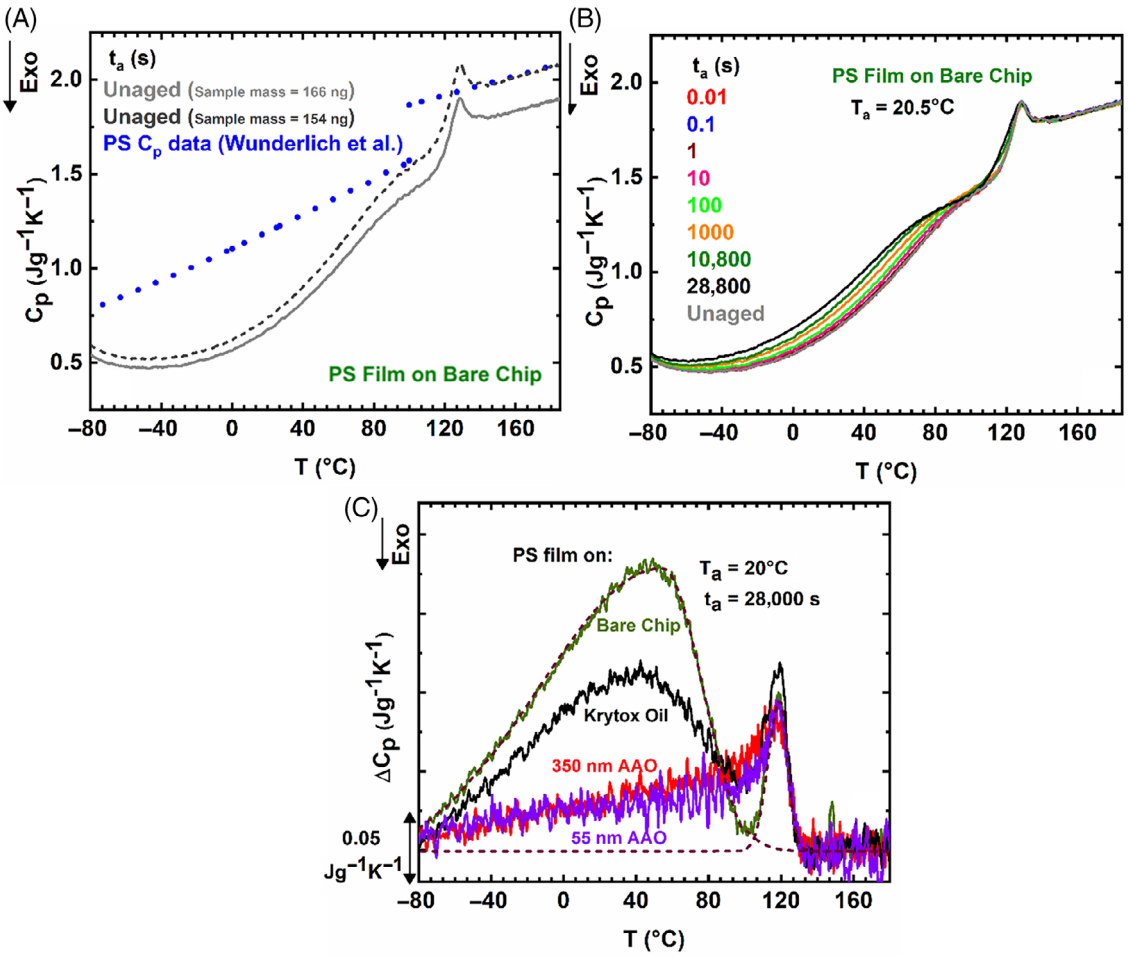

FIGURE 1 (A) Specific heat capacities of unaged polystyrene on a bare chip (using sample mass obtained using ΔC_p in light gray and using sample mass obtained using liquid state heat capacity in dark gray) compared with Gaur and Wunderlich's specific heat data of amorphous polystyrene[14] (blue solid circles). (B) Specific heat capacities of polystyrene on a bare chip at $T_a = 20.5°C$ as a function of aging time. (C) Excess specific heat of polystyrene film aged for 8 h relative to the unaged sample on different substrates at $T_a = 20.5°C$ with the dashed lines showing the deconvolution of the two peaks for the case of the bare chip.

$$\int_{T_f}^{T\gg T_g} (\dot{Q}_l - \dot{Q}_g)dT = \int_{T\ll T_g}^{T\gg T_g} (\dot{Q} - \dot{Q}_g)dT, \quad (3)$$

$$\int_{T_f}^{T\gg T_g} (\dot{Q}_l - \dot{Q})dT = 0, \quad (4)$$

where $\dot{Q}$, $\dot{Q}_l$, and $\dot{Q}_g$ are the sample heat flow, liquid heat flow, and glass heat flow, respectively. The fictive temperature, T_f, which is a measure of glass structure, is related to the enthalpy difference obtained in Equation (2):

$$\Delta H = -\int_{T_{fo}}^{T_f} \Delta C_p dT, \quad (5)$$

where T_{fo} is the initial or reference fictive temperature of the unaged glass at a reference cooling rate of 1000 K/s, and ΔC_p is the temperature dependent step change in the heat capacity at T_g from Equation (1). As aging increases and the enthalpy change increases, the fictive temperature decreases. Theoretically, on aging, the fictive temperature will equal the aging temperature when the material reaches equilibrium, as defined by the extrapolated liquid line.

The cooling rate dependence of the fictive temperature T_f' can be described by the Williams-Landel-Ferry (WLF)[22] equation:

$$\log\left(\frac{q_o}{q}\right) = \frac{-C_1(T_g - T_{g,\text{ref}})}{C_2 + (T_g - T_{g,\text{ref}})} \quad (6)$$

where $T_{g,\text{ref}}$ is the reference glass transition temperature obtained at a cooling rate of $q_o = 0.1$ K/s, T_g is the glass transition temperature at a particular cooling rate,

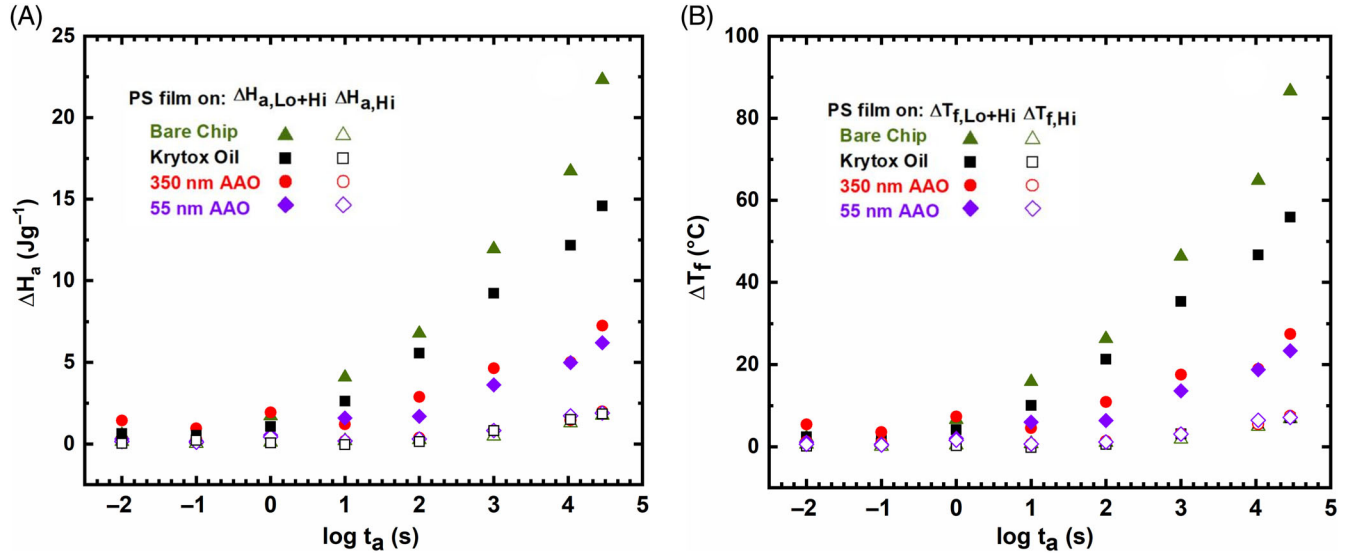

FIGURE 2 (A) Enthalpy of aging (ΔH_a) as a function of aging time for polystyrene on different substrates. (B) The change in fictive temperature ($\Delta T_f = T_{fo} - T_f(t_a)$) as a function of aging time for polystyrene on different substrates. The solid symbols represent ΔH_a and ΔT_f that were obtained inclusive of both low- and high-temperature endotherms and the open symbols represent those obtained only from high-temperature endotherms.

equivalent to T_f' measured at that cooling rate, and C_1 and C_2 are WLF constants.

The fictive temperatures were corrected for dynamic temperature gradients according to the method suggested by Schawe.[23] The correction is obtained from average of the difference between T_g obtained on cooling at 1000 K/s and T_f obtained on heating at 1000 K/s. The correction was subtracted from fictive temperatures obtained for other cooling rates and the values are 2.2°C, 0.4°C, 3.8°C, and 6.1°C for PS on bare, Krytox, 350 nm AAO, and 55 nm AAO, respectively. Corrections of this magnitude are normal for differences between chips in Flash DSC.[24,25] In addition, an isothermal temperature correction factor of 0.5 K was also applied for aging temperatures as reported in previous studies.[24,25]

4 | RESULTS

4.1 | Aging of polystyrene

The specific heat capacity as a function of temperature for the bulk unaged polystyrene film is shown in Figure 1A, along with the values from Gaur and Wunderlich.[14] Two curves are shown for our data, one using the mass obtained by matching the step change in the heat capacity at T_g (166 ng), which shows a specific heat some 9% lower than the literature value in the liquid state, and the other where the mass was obtained from matching the heat capacity with the literature in the liquid state (154 ng). For the latter case, the glass line matches also agrees well with Gaur and Wunderlich[14] but only to approximately 10 K below T_g. At lower temperatures, there is clearly curvature in our measurements, the origin of which is the focus of this paper. Our error of 9% in the sample mass obtained from matching ΔCp is of similar magnitude to the errors obtained by Quick et al.[26] for Flash DSC measurements of lead with mass obtained from the heat of fusion. We obtain an error of similar magnitude for our indium sample, whose specific heat is compared to the literature in Appendix S1; and a slightly larger error for gold, also shown compared to the literature in Appendix S1.

The influence of aging at 20.5°C on the specific heat of the same bulk polystyrene film on the bare chip is shown in Figure 1B as a function of aging time. The most obvious change with aging time is the increase in specific heat between −80°C and 80°C, which can be interpreted as the growth of a broad low-temperature endothermic peak. In addition, there is a small shoulder that appears on the enthalpy overshoot at T_g (in the vicinity of 120°C) which increases with increasing aging at 20.5°C. These two effects can be clearly observed in the differential or excess specific heat of the sample aged for 8 h at 20.5°C relative to the unaged sample, as shown in Figure 1C for the four substrate conditions, that is, polystyrene sample on bare chip, Krytox oil, 350 nm AAO template, and 55 nm AAO template. The high-temperature enthalpy overshoot at T_g for all four samples have similar devitrification temperatures (~100°C), peak temperatures (~120°C), and peak areas irrespective of the substrate. On the other hand, the low-temperature endotherms have peak areas that strongly depend on the substrate, with the polystyrene film on the bare chip having the largest area.

The changes in specific heat that occur with aging are quantified by the enthalpy change on aging (ΔH_a) determined using Equation (3). The results are shown for the four substrate conditions as a function of aging time in Figure 2A, with open symbols showing the result when we only considered the endothermic overshoot at T_g ($\Delta H_{a,\mathrm{Hi}}$) and solid symbols obtained by considering both the overshoot at T_g and the broad low-temperature endotherm ($\Delta H_{a,\mathrm{Lo+Hi}}$). The corresponding changes in fictive temperature (determined using Equation (5)) are shown in Figure 2B, again for results considering only the high-temperature endotherm at T_g ($\Delta T_{f,\mathrm{Hi}}$) and for results when both high- and low-temperature endotherms are considered ($\Delta T_{f,\mathrm{Lo+Hi}}$). The enthalpy change on aging determined from the high-temperature peaks ($\Delta H_{a,\mathrm{Hi}}$) are consistent with one another for different substrates at a given aging time; for example, from the high-temperature peak, the average changes in enthalpy and fictive temperature for a 1.3 μm thick polystyrene that has been aged for 8 h at 20.5°C on different substrates are $\Delta H_{a,\mathrm{Hi}} = 2.1 \pm 0.1$ J/g and $\Delta T_{f,\mathrm{Hi}} = 7.1 \pm 0.3$°C, which agree quite well to those observed in recent studies.[27,28] On the other hand, when both the high- and low-temperature endotherms are considered, the results vary dramatically depending on the substrate. The largest enthalpy and fictive temperature changes are for the polystyrene film on the bare chip, where $\Delta H_{a,\mathrm{Lo+Hi}}$ is 22.5 J/g and the corresponding $\Delta T_{f,\mathrm{Lo+Hi}}$ is approximately 90°C, three time larger than the changes for the polystyrene film on the 55 nm AAO.

4.2 | Cooling rate dependence of polystyrene

The influence of cooling rate on the specific heat of the bulk polystyrene film on the bare chip is shown in Figure 3 for cooling rates from 0.1 to 1000 K/s, with Figure 3A showing the results when scanned to 30°C and Figure 3B showing the results when scanned to −80°C. In both the cases, the enthalpy overshoots at T_g shift to higher temperatures and are larger in magnitude with decreasing cooling rate. The experimental data obtained for the two cases have similar devitrification points with well superposed liquid lines, whereas glass lines are well superposed only in the case of cooling to 30°C. In the case of scanning to −80°C, glass lines do not superpose and a broad low-temperature endothermic peak, similar to what was observed in the case of the aforementioned aging experiments, appears to evolve and grow in magnitude with decreasing cooling rate.

It is well known that the glass transition temperature (T_g) and the equivalent limiting fictive temperature (T_f') decrease as cooling rate decreases. The T_f' values as a function of cooling rate for different substrates and scanning to different temperatures are shown in Figure 4. The fictive temperatures are calculated using Moynihan's or Richardson's method (Equations (3) and (4), respectively) for the data shown in Figure 3A scanned to 30°C where there is no low-temperature endotherm and shown as open symbols. For the data scanned to −80°C (solid symbols), only the high-temperature overshoot was considered for this analysis. For the four different samples (on different substrates), the absolute T_f' values have a standard deviation of 3.5 K and are all within 5 K of our previous data. This is well within the expectation for Flash DSC; for example, in previous work,[25] we found that T_f' values for the same nominal polystyrene sample on four different chips varied by as much as 4.6°C. The values of T_f as a function of cooling rate are also well described by the Williams-Landel-Ferry (WLF) equation and are plotted as solid lines, and the parameters are $C_1 = 18.9$, $C_2 = 55.3$ K, which are comparable to values previously reported by our laboratory.[17,18,25,28,29]

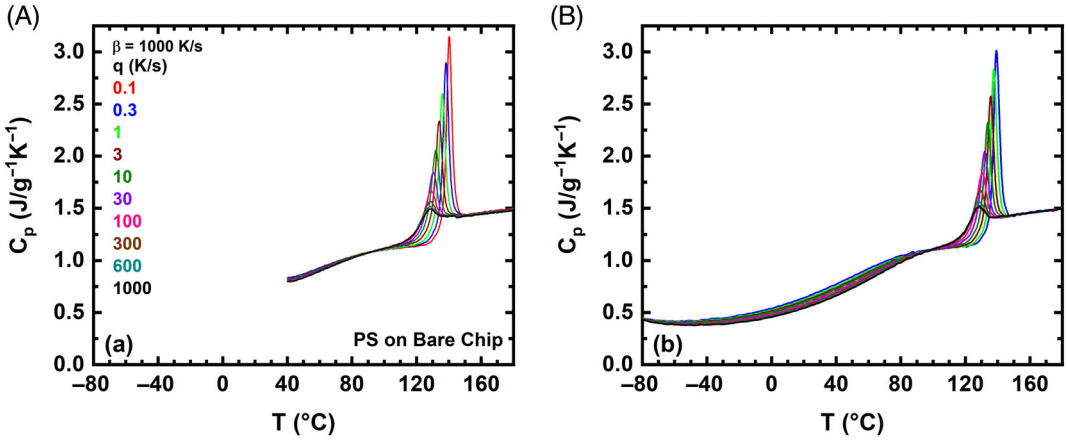

FIGURE 3 Evolution of DSC scans of polystyrene on the bare chip as a function of different cooling rates when scanned to (A) 30°C and (B) −80°C.

The data in Figure 4 considered only the endothermic overshoot at T_g, and, for the data scanned to a low-temperature endpoint of −80°C, excluded contributions from the low-temperature endotherm. The magnitude of the contributions from the endotherms at low-temperature versus high-temperature can be qualitatively observed in Figure 5A, where the excess specific heat data are plotted versus temperature for scanning at the slowest rate of 0.1 K/s relative to that at 1000 K/s for all four samples having various substrate conditions. Similar to the isothermal aging data shown earlier in Figure 1C, the largest low-temperature endotherm is observed in the case of the polystyrene film on the bare chip. As an aside, we note that scanning slowly is analogous to aging with the difference being that the relaxation during a cooling scan is taking place non-isothermally as opposed to isothermally at T_a. The enthalpy changes (from Equation (3)) from the excess specific heat data are shown in Figure 5B as a function of cooling rate for all four substrates with open symbols showing the results when only the high-temperature endothermic step change at T_g is accounted for, whereas the solid symbols show the results when both the low-temperature and high-temperature peaks are considered. For the former case, similar enthalpy values are observed, independent of substrate condition and for the slowest cooling rate of 0.1 K/s, $H_{0.1}$-$H_{1000,Hi} = 3.4 \pm 0.2$ J/g for all four samples. This is in spite of the small change in the overshoot at T_g, with substrate condition because it is compensated by differences in the undershoot just preceding the overshoot. On the other hand, the same quantity differs considerably when the low-temperature endotherm is considered with values differing by a factor of three (similar to the isothermal aging results) with the polystyrene on the bare chip having the largest value of $H_{0.1}$-$H_{1000,Lo+Hi}$ and that on the 55 nm AAO having the lowest. The same trends are shown in Figure 5C for the limiting fictive temperature, with the average $\Delta T_{f,Hi} = 13.1 \pm 0.8$ for the 0.1 K/s cooling rate, independent of substrate condition, whereas $\Delta T_{f,Lo+Hi}$ varies by a factor of three, similar to enthalpy change, $H_{0.1}$-$H_{1000,Lo+Hi}$.

In the previous sections, we have seen that the magnitude of the low-temperature endotherm of the polystyrene films differs with changes in underlying substrate, whereas the overshoot at T_g does not, suggesting a potential artifact rather than a relaxation inherent to the material. To further probe this possibility, similar aging and cooling rate dependent experiments are performed on indium and gold, crystalline metals in solid state with no

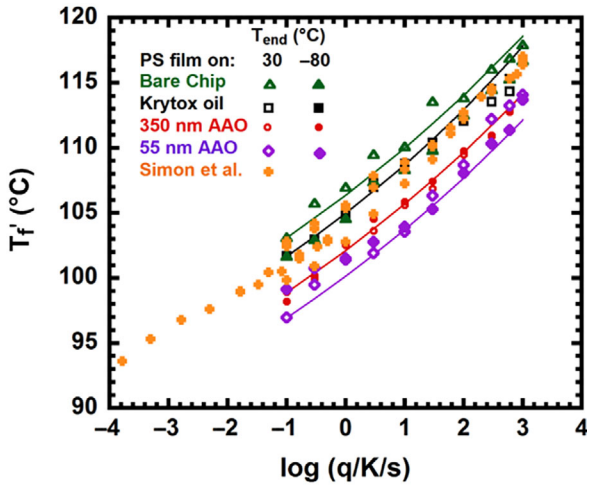

FIGURE 4 Limiting fictive temperatures as a function of cooling rate for polystyrene on different substrates when scanned to 30°C (open symbols) and −80°C (closed symbols) considering only the endothermic overshoot associated with T_g. Also shown (orange symbols) are results from our earlier studies.[17,18,25,28,29]

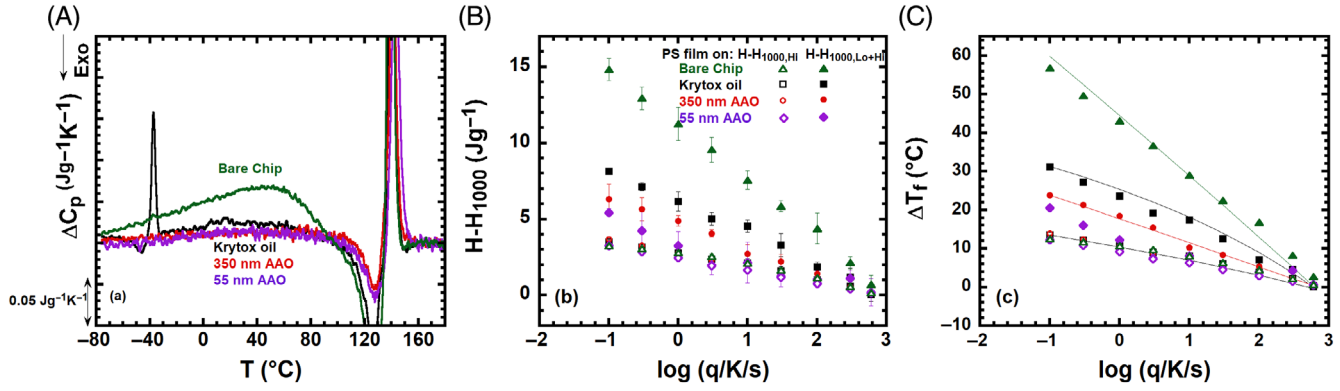

FIGURE 5 (A) Excess specific heat scans of polystyrene at a cooling rate of 0.1 K/s with 1000 K/s as the reference curve for various substrate conditions. (B) The change in enthalpy and (C) the change in fictive temperature as a function of cooling rate. The open and solid symbols correspond to values excluding and including the contribution from the low-temperature endotherm, respectively. The enthalpy recovery peak at the Krytox Tg near −40°C is not included in the area calculation.

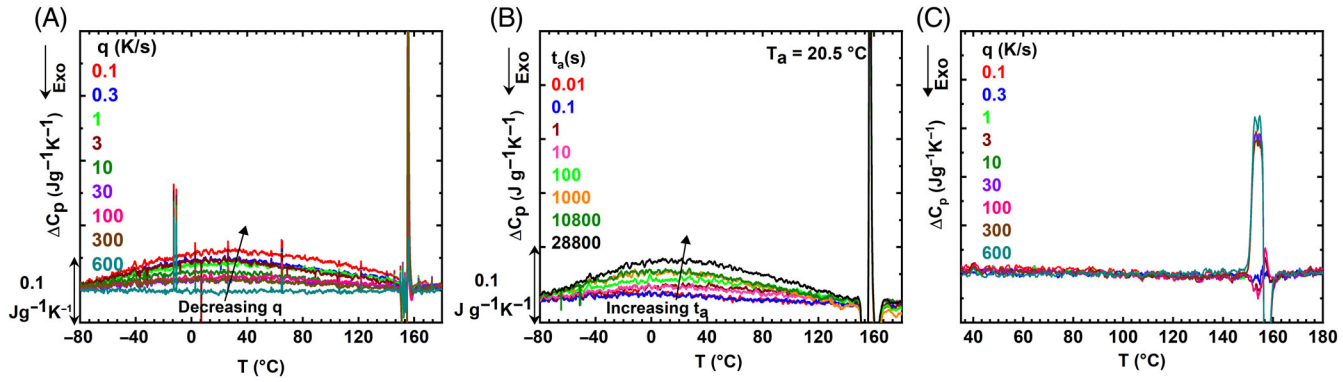

FIGURE 6 (A) Excess specific heat for indium at various cooling rates with respect to 1000 K/s. (B) Excess specific heat for indium at various aging times for aging at 20.5°C with respect to the unaged scan. (C) Excess specific heat for indium at various cooling rates with respect to 1000 K/s for cooling to an endpoint temperature of 30°C, as opposed to −80°C in the case of (A) and (B).

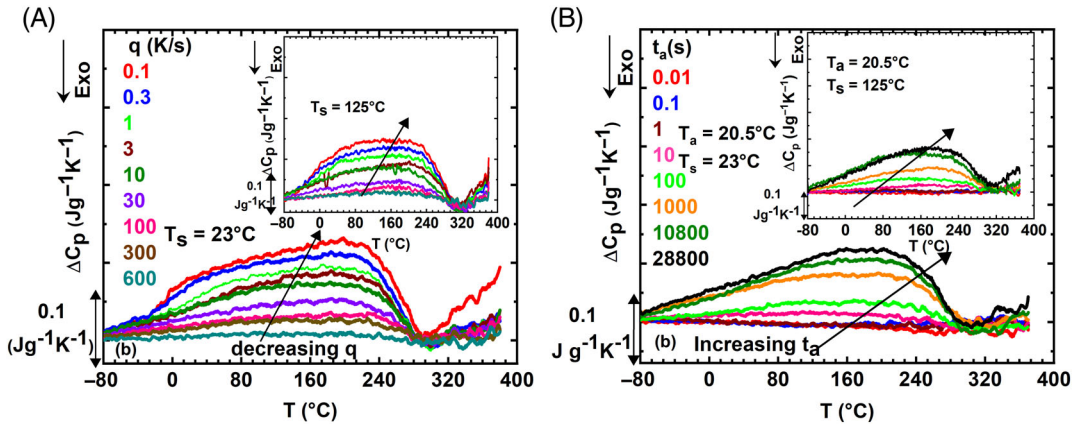

FIGURE 7 Excess specific heat as a function of (A) cooling rate and (B) aging time for aging at 20.5°C for gold vapor deposited at a substrate temperature of 23°C. The insets show the results for deposition at 125°C.

known relaxation mechanisms in the temperature regime probed.

Heat flow scans of 1 μm thick indium at a heating rate of 1000 K/s from −80°C after cooling at various rates in the range of 0.1–1000 K/s, and after aging at 20.5°C for various times in the range of 0.01 s to 8 h are obtained and converted to excess heat flow scans with respect to a reference heat flow scan at 1000 K/s, as shown in Figure 6A,B. The evolution of a low-temperature endotherm is clearly observed with decreasing cooling rate and increasing aging time, whereas the melting transition at 156.6°C is unaffected. On the other hand, when scans are only made to the low-temperature end point of 30°C, the data superpose from 30°C to 120°C within the noise of the measurements, as shown in Figure 6C.

The cooling rate- and aging time-dependent excess specific heats of 50 nm vapor deposited gold are shown in Figure 7A,B for material deposited at a substrate temperature of 23°C; similar results with slightly larger areas are obtained for material deposited with a substrate temperature of 125°C as shown in the insets. The excess specific heat exhibits a similar low-temperature broad endotherm, as seen for both polystyrene films and indium when they are scanned to the low endpoint temperature of −80°C. For gold, the endotherms commence at the lowest temperatures and grow in magnitude as temperature increases, similar to the case of indium, but for gold, the endotherms appear to end at ~300°C. In the case of indium, the low-temperature endotherm ends just before reaching T_m, which is the zero-stress condition for the crystalline material; similarly, for polystyrene, when the low-temperature endotherm is present (i.e., when the material is cooled to −80°C), it ends just before the undershoots and overshoots associated with T_g, which is again expected to be the zero-stress state. For vapor-deposited gold, on the other hand, we might expect the zero-stress state to be near the deposition temperature (i.e., where the solid was formed); however, although we

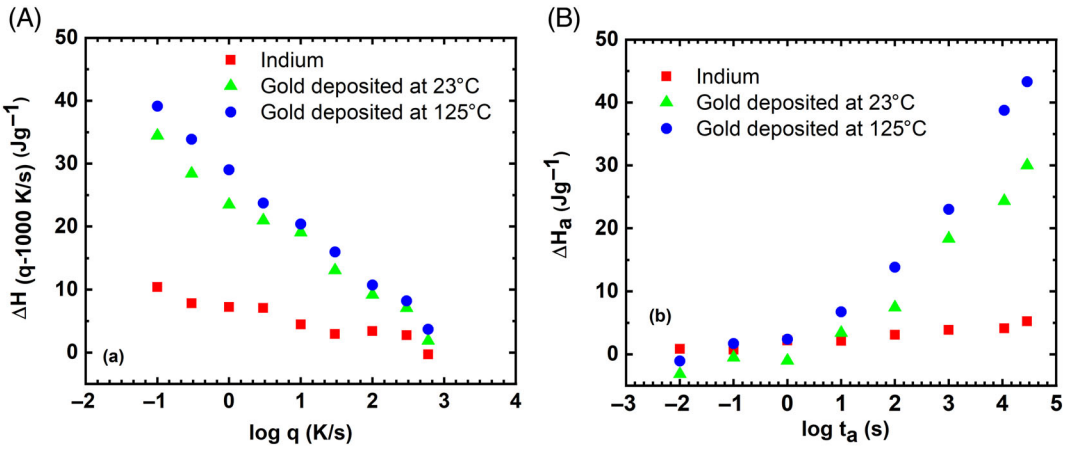

FIGURE 8 Change in enthalpy for indium, gold deposited at 23°C and at 125°C as a function of (A) cooling rate and (B) aging time for aging at 25°C.

do observe the growth of a larger endothermic peak for deposition at 125°C, the temperature at which the peak ends is only slightly elevated.

The enthalpy changes associated with the low-temperature endotherm as a function of cooling rate and aging time for the indium and gold samples are shown in Figure 8A,B, respectively. As mentioned previously, the enthalpies increase with decreasing cooling rate and increase with increasing aging time, as was observed for polystyrene. The enthalpy is highest for the gold, vapor deposited at $T_s = 125$°C and lowest for indium. In cases of the slowest cooling rate (0.1 K/s) and highest aging time (8 h), the enthalpy is in the range of 40–45 J/g for both gold samples and 6–10 J/g for indium; in case of polystyrene on the bare chip the enthalpies of the low-temperature endotherm in case of aging (8 h) and cooling rate (q = 0.1 K/s) experiments are in a similar range, being approximately 20 and 12.5 J/g, respectively, when scans are performed to −80°C and both high- and low-temperature endotherms are considered.

5 | DISCUSSION

The effect of different cooling rates on limiting fictive temperature for polystyrene bulk film was reported previously by Simon and co-workers where the material was scanned to a low temperature ranging from 25°C to 50°C, depending on the study.[16–18,29] Here, the comparison of the heat flow curves and resulting values of the fictive temperature by scanning to two different end temperatures, −80°C and 30°C, for micron-scale PS films on four different substrates is investigated. The resulting T_f values by Moynihan's or Richardson's method for the two different end temperatures are comparable with previous results[16–18,29] for the samples cooled to an end temperature above 25°C, independent of substrate conditions, and a similar result is obtained when only the endothermic overshoot associated with T_g is analyzed in the case of the end temperature of −80°C. Similarly, the resulting enthalpy values by integrating the high-temperature area (glass transition region) from 110°C to 160°C for polystyrene on different substrates are also comparable with an average value of 3.44 ± 0.18 J/g at a cooling rate of 0.1 K/s, which is slightly lower than the average value (4.18 ± 0.43 J/g) from previous studies.[16–18,29] In case of aging experiments at 20.5°C, the enthalpy of aging of the glass transition area (110°C–160°C) also are in good agreement with an average value of 1.62 ± 0.14 J/g for an aging time of 8 h across different substrates. On the other hand, the resulting enthalpy values that include the low-temperature endotherm are different for all of the substrates studied and vary by as much as ~200% for the cooling-rate dependent experiments and ~300% for aging experiments. In both types of experiments the largest area is observed for polystyrene on the bare chip, and smallest area is observed for polystyrene film on 55 nm AAO pores. One potential explanation is that the difference across substrates is due to differences in the magnitude of stresses arising from the interaction between the sensor membrane and the sample when cooled to low temperatures rather than to relaxations inherent to the material itself. The fact that the low-temperature endotherms, both cooling rate dependent and aging time dependent, are also observed for indium and gold, which have no fast relaxations in this temperature range, supports the supposition that the low-temperature endotherm is an artifact.

The idea of correlating the low-temperature endotherms observed on Flash DSC with a fast relaxation

mechanism was first reported by Cangialosi and co-workers,[3] where polystyrene nanospheres aged at low temperatures for longer times exhibited a low-temperature endotherm which was interpreted to be the fast step in a two-step structural recovery process. In addition, they reported that the low-temperature endotherm was not observed for bulk nanospheres, contrary to what was observed here for 1.3 μm (bulk) polystyrene films. Cangialosi and co-workers also reported the appearance of low-temperature endotherms[1] for different micron sized poly(4-tert-butylstyrene) films as a function of cooling rates and thicknesses of micron-scale films using conventional DSC; thinner micron-scale films showed larger low-temperature endothermic overshoots and hence an 80°C change in T_f for 2.5 μm thick film.[1] The large change in T_f was attributed to the fast relaxation contributed by the low-temperature endotherm; however, bulk-like mobilities were reported for all micron-scale poly(4-tert-butylstyrene) films irrespective of the large changes in T_f.[1] Similar changes in T_f are reported in the present work using Flash DSC with $\Delta T_{f,\mathrm{Hi+Lo}}$ being as large as ~60°C at 0.1 K/s and as large as ~90°C for an 8 h aged sample at 20°C, with the magnitude of $\Delta T_{f,\mathrm{Hi+Lo}}$ following the order of bare chip > Krytox Oil >350 nm AAO > 55 nm AAO. Interestingly, when the low-temperature endotherm is included in the calculation, the reductions in fictive temperatures observed both here and from Cangialosi and co-workers[1] (of 80°C–90°C) are larger than the fictive temperature changes observed in 20-million-year aged amber[30] and ultrastable molecular and polymer glasses,[31–33] a highly suspect result.

Thermal residual stresses are known to occur as a result of differential thermal expansion between two materials in a layer or sandwich configuration, with such stresses being zero at the stress-free temperature. In the case of the Flash DSC setup, the sensor is a 2 μm silicon nitride membrane with low thermal expansion and high modulus, coated with a thin layer of aluminum for enhanced heat transfer, whereas the polystyrene, indium, and gold samples all have higher thermal expansion coefficients and lower moduli. Thus, it is expected that the samples will be constrained from shrinking and will experience a tensile force during cooling, whereas the sensor will experience the opposite; and then, on heating, the stresses would be relieved. The strain energy for this biaxial deformation is given by $\Delta U = (\alpha - \alpha_{\mathrm{substrate}})E\Delta T/(1-\nu)/2$, where $\alpha - \alpha_{\mathrm{substrate}}$ is the differential linear thermal expansion coefficient between the sample and the sensor substrate, E is the biaxial modulus, ΔT is the temperature change from the stress-free temperature, considered to be T_g for polystyrene, T_m for indium, and T_s for gold, and ν is the Poisson's ratio. The strain energies on cooling to −80°C are on the order of ~34 J/g for polystyrene, 13 J/g for indium, and 10 J/g for gold. However, these thermal residual stresses are elastic and are not anticipated to change significantly with cooling rate or aging time, and thus, although they seem to be of the right order of magnitude, we do not see that they can account for the evolution of the low-temperature endotherm that is observed in this work as a function of cooling rate and aging time.

A final speculation is that the low-temperature endotherm could be due to water that adsorbs on the sample or sensor at low temperatures and then desorbs during the heating scan giving the broad low-temperature endotherm. Assuming that the heat of desorption is 105 J/g (that for desorption of water from gold), approximately 40 ng of water would need to be adsorbed during slow cooling at 0.1 K/s to give rise to the endothermic peak area observed for gold at the slowest cooling rates; this would require, at the typical nitrogen purge rates of 20 ml/min, a water content of at least 0.0015% in the nitrogen purge. Such a water level is well within expectations, with levels of 0.018% having been measured in a full compressed nitrogen tank and 10 times that level in an almost-empty tank.[34] Water adsorption/desorption also has the potential to explain why broad endotherms have been observed in conventional DSC. The influence of water adsorption at low temperature followed by desorption during the heating scan will be investigated in future work for both Flash and conventional DSC.

6 | CONCLUSIONS

Flash differential scanning calorimetry is used to study the origin of a low-temperature endotherm for 1.3 μm polystyrene films with four substrate conditions, as well as for indium and vapor-deposited gold. A low-temperature broad endotherm is observed to evolve with decreasing cooling rate and increasing aging time at 20.5°C for all samples when scanned to the low endpoint temperature of −80°C. On the other hand, the low-temperature endotherms are non-existent for samples when the low endpoint temperature was limited to 30°C. In addition, the area of the low-temperature endotherm for polystyrene is found to depend on the substrate conditions, whereas the high-temperature endotherm in the vicinity of T_g (i.e., the endothermic overshoot at T_g) is found to be independent of the substrate. The inconsistency in the magnitude of areas pertinent to the low-temperature endotherm, as well as their presence in the case of indium and gold samples, suggests that the low-temperature endotherm is not a material property and not related to a fast relaxation. Rather, we suggest that the evolution of what appears to be a low-temperature endotherm is an artifact arising either from residual

stresses or from desorption of water adsorbed at low temperature.

ACKNOWLEDGMENTS

Funding from NSF DMR-2004960 and DMR-2141221 is gratefully acknowledged. The authors also acknowledge Dr. Qi Li for his help with AFM measurements to determine polystyrene film thickness.

DATA AVAILABILITY STATEMENT

Data will be supplied upon reasonable request; email slsimon@ncsu.edu.

ORCID

Sindee L. Simon https://orcid.org/0000-0001-7498-2826

REFERENCES

[1] X. Monnier, D. Cangialosi, *Phys. Rev. Lett.* **2018**, *121*(13), 137801.
[2] X. Monnier, D. Cangialosi, *Thermochim. Acta* **2019**, *677*, 60.
[3] N. G. Perez-De-Eulate, D. Cangialosi, *Macromolecules* **2018**, *51*(9), 3299.
[4] V. M. Boucher, D. Cangialosi, A. Alegría, J. Colmenero, *PCCP* **2017**, *19*(2), 961.
[5] N. G. Perez-De Eulate, D. Cangialosi, *PCCP* **2018**, *20*(18), 12356.
[6] V. M. Boucher, D. Cangialosi, A. Alegría, J. Colmenero, *J. Chem. Phys.* **2017**, *146*(20), 203312.
[7] C. Fischer, A. Seefried, D. Drummer, *Polym. Eng. Sci.* **2017**, *57*(4), 450.
[8] K. Jariyavidyanont, J. L. Williams, A. M. Rhoades, I. Kuehnert, W. Focke, R. Androsch, *Polym. Eng. Sci.* **2018**, *58*(7), 1053.
[9] M. A. Kolmangadi, P. Szymoniak, R. Zorn, M. Bohning, M. Wolf, M. Zamponi, A. Schonhals, *Polym. Eng. Sci.* **2022**, *62*(7), 2143.
[10] A. Toda, M. Konishi, *Thermochim. Acta* **2014**, *589*, 262.
[11] M. R. Pallaka, D. K. Unruh, S. L. Simon, *Thermochim. Acta* **2018**, *663*, 157.
[12] P. Cebe, B. P. Partlow, D. L. Kaplan, A. Wurm, E. Zhuravlev, C. Schick, *Thermochim. Acta* **2015**, *615*, 8.
[13] Y. P. Koh, G. B. McKenna, S. L. Simon, *J. Polym. Sci. B: Polym. Phys.* **2006**, *44*(24), 3518.
[14] U. Gaur, B. Wunderlich, *J. Phys. Chem. Ref. Data* **1982**, *11*, 313.
[15] Y. Takahashi, H. Akiyama, *Thermochim. Acta* **1986**, *109*(1), 105.
[16] Y. P. Koh, S. L. Simon, *J. Polym. Sci. B Polym. Phys.* **2008**, *46*(24), 2741.
[17] E. Lopez, S. L. Simon, *Macromolecules* **2016**, *49*(6), 2365.
[18] S. Y. Gao, Y. P. Koh, S. L. Simon, *Macromolecules* **2013**, *46*(2), 562.
[19] http://webbook.nist.gov/chemistry/.
[20] C. T. Moynihan, P. B. Macedo, C. J. Montrose, P. K. Gupta, M. A. DeBolt, J. F. Dill, B. E. Dom, P. W. Drake, A. J. Easteal, P. B. Elterman, *Ann. N. Y. Acad. Sci.* **1976**, *279*(1), 15.
[21] M.-J. Richardson, N. Savill, *Polymer* **1975**, *16*(10), 753.
[22] M. L. Williams, R. F. Landel, J. D. Ferry, *J. Am. Chem. Soc.* **1955**, *77*(14), 3701.
[23] J. E. Schawe, *Thermochim. Acta* **2015**, *603*, 128.
[24] Y. P. Koh, S. Y. Gao, S. L. Simon, *Polymer* **2016**, *96*, 182.
[25] Y. P. Koh, L. Grassia, S. L. Simon, *Thermochim. Acta* **2015**, *603*, 135.
[26] C. Quick, J. Schawe, P. Uggowitzer, S. Pogatscher, *Thermochim. Acta* **2019**, *677*, 12.
[27] L. Grassia, Y. P. Koh, M. Rosa, S. L. Simon, *Macromolecules* **2018**, *51*(4), 1549.
[28] Y. P. Koh, S. L. Simon, *J. Chem. Phys.* **2017**, *146*(20), 203329.
[29] S. Y. Gao, S. L. Simon, *Thermochim. Acta* **2015**, *603*, 123.
[30] J. Zhao, S. L. Simon, G. B. McKenna, *Nat. Commun.* **2013**, *4*, 1783.
[31] S. F. Swallen, K. L. Kearns, M. K. Mapes, Y. S. Kim, R. J. McMahon, M. D. Ediger, T. Wu, L. Yu, S. Satija, *Science* **2007**, *315*(5810), 353.
[32] H. Yoon, Y. P. Koh, S. L. Simon, G. B. McKenna, *Macromolecules* **2017**, *50*(11), 4562.
[33] H. Yoon, G. B. McKenna, *Sci. Adv.* **2018**, *4*(12), eaau5423.
[34] A. C. Walker, E. J. Ernst Jr., *Ind. Eng. Chem. Anal. Ed.* **1930**, *2*(2), 139.

SUPPORTING INFORMATION

Additional supporting information can be found online in the Supporting Information section at the end of this article.

How to cite this article: M. R. Pallaka, R. Bari, S. L. Simon, *Polym. Eng. Sci.* **2022**, *62*(9), 3059. https://doi.org/10.1002/pen.26102